Entanglement of Purification in Many Body Systems and Symmetry Breaking

Arpan Bhattacharyya,[1] Alexander Jahn,[2] Tadashi Takayanagi,[1,3] and Koji Umemoto[1]
[1]*Center for Gravitational Physics, Yukawa Institute for Theoretical Physics, Kyoto University, Kitashirakawa Oiwakecho, Sakyo-ku, Kyoto 606-8502, Japan*
[2]*Dahlem Center for Complex Quantum Systems, Freie Universität Berlin, 14195 Berlin, Germany*
[3]*Kavli Institute for the Physics and Mathematics of the Universe (WPI), University of Tokyo, Kashiwa, Chiba 277-8582, Japan*

(Received 4 March 2019; published 22 May 2019)

We study the entanglement of purification (EOP), a measure of total correlation between two subsystems A and B, for free scalar field theory on a lattice and the transverse-field Ising model by numerical methods. In both of these models, we find that the EOP becomes a nonmonotonic function of the distance between A and B when the total number of lattice sites is small. When it is large, the EOP becomes monotonic and shows a plateaulike behavior. Moreover, we also show that the original reflection symmetry which exchanges A and B can get broken in optimally purified systems. We provide an interpretation of our results in terms of the interplay between classical and quantum correlations.

DOI: 10.1103/PhysRevLett.122.201601

The entanglement entropy (EE) is a unique measure of quantum entanglement for pure states [1]. Decomposing a total quantum system into two subsystems A and B, the EE is defined as $S_A = -\mathrm{Tr}[\rho_A \log \rho_A]$, where the reduced density matrix is $\rho_A \equiv \mathrm{Tr}_B |\Psi\rangle_{AB}\langle\Psi|_{AB}$, and $|\Psi\rangle_{AB}$ describes a pure state. The EE helps us to extract essential properties of quantum field theories [2,3], especially conformal field theories (CFTs) [4]. It has recently played an important role in the context of the anti–de Sitter space/conformal field theory (AdS/CFT) correspondence (or holography) [5], due its simple geometrical interpretation in gravity [6,7].

Quantities such as entanglement of formation and squashed entanglement extend EE to mixed states, where the EE itself is not a good measure of quantum entanglement or classical correlations (refer to, e.g., a comprehensive review [8]). However, such quantities often require a minimization over infinitely many quantum states and are thus computationally challenging in quantum field theory, leading to a scarcity of results.

This Letter provides a first step toward such a minimization. We will study entanglement of purification (EOP) $E_P(\rho_{AB})$ [9,10], a simpler version of more complicated mixed state entanglement measures and defined as follows: Consider a purification $|\Psi\rangle_{A\tilde{A}B\tilde{B}}$ of a mixed state ρ_{AB}, i.e., a pure state in an enlarged Hilbert space $\mathcal{H}_A \otimes \mathcal{H}_B \to \mathcal{H}_A \otimes \mathcal{H}_B \otimes \mathcal{H}_{\tilde{A}} \otimes \mathcal{H}_{\tilde{B}}$ with a constraint

$$\mathrm{Tr}_{\tilde{A}\tilde{B}}[|\Psi\rangle_{A\tilde{A}B\tilde{B}}\langle\Psi|_{A\tilde{A}B\tilde{B}}] = \rho_{AB}. \tag{1}$$

EOP is given by the minimal EE $S_{A\tilde{A}}$ over all purifications $|\Psi\rangle_{A\tilde{A}B\tilde{B}}$

$$E_P(\rho_{AB}) = \min_{|\Psi\rangle_{A\tilde{A}B\tilde{B}}} S_{A\tilde{A}}. \tag{2}$$

EOP is a measure of total correlation between the two subsystems A and B: it vanishes only for product states and monotonically decreases under local operations, while its regularization possesses an operational meaning in terms of Einstein-Podolsky-Rosen (EPR) pairs [9]. Moreover, an AdS/CFT-based geometric interpretation was conjectured [11,12], supported by CFT approaches for specific examples [13], and actively studied [14–35], motivating a field-theoretic treatment. Earlier work on EOP for free scalar field theory has been performed for small subsystems [36].

In this Letter, we numerically study the EOP in free scalar field theory for larger subsystems assuming a Gaussian ansatz, as well as in the transverse-field Ising chain. Both models exhibit intriguing nonmonotonic and plateaulike behavior of EOP with respect to the distance between the subsystems. Moreover, we observe a breaking of the Z_2 reflection symmetry that exchanges $A\tilde{A}$ and $B\tilde{B}$ for an optimal purification, reminiscent of spontaneous symmetry breaking and unobserved in previous work [36].

First, consider a lattice free scalar field theory in $1+1$ dimensions, defined by the Hamiltonian

$$H = \frac{1}{2}\int_{-\infty}^{\infty} dx[\pi^2 + (\partial_x\phi)^2 + m^2\phi^2]. \tag{3}$$

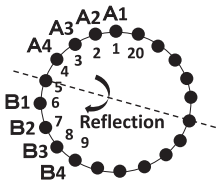

FIG. 1. An example of the setup for our lattice model with $N = 20$ and $|A| = |B| = 4$. The distance between A and B is $d = 1$. There is a Z_2 reflection symmetry.

The ground state wave function Ψ_0 for this theory is Gaussian [2,36,37]

$$\Psi_0[\phi] = \mathcal{N}_0 e^{-\frac{1}{2}\sum_{n,n'=1}^{N}\phi'_n W_{nn'}\phi'_{n'}} \equiv \mathcal{N}_0 e^{-\frac{1}{2}\phi^T W\phi}. \quad (4)$$

The matrix W is defined by

$$W_{nn'} = \frac{1}{N}\sum_{k=1}^{N}\sqrt{m^2a^2 + 4\sin^2\left(\frac{\pi k}{N}\right)}\, e^{[2\pi ik(n-n')/N]}, \quad (5)$$

where N is the total number of lattice sites. We set the lattice spacing $a = 1$. Notice that W is symmetric and real valued. We consider masses between $m = 10^{-1}$ and $m = 10^{-4}$ near the conformal (massless) limit.

We divide the total Hilbert space into three parts $\mathcal{H}_{\text{tot}} = \mathcal{H}_A \otimes \mathcal{H}_B \otimes \mathcal{H}_C$ (Fig. 1). We denote the number of lattice sites in A, B by $|A|, |B|$ and the distance between them by d. Then Eq. (4) is written as

$$\Psi_0[\phi] = \mathcal{N}_0 \exp\left[-\frac{1}{2}\begin{pmatrix}\phi_{AB}\\ \phi_C\end{pmatrix}^{\mathrm{T}}\begin{pmatrix}P & Q\\ Q^{\mathrm{T}} & R\end{pmatrix}\begin{pmatrix}\phi_{AB}\\ \phi_C\end{pmatrix}\right], \quad (6)$$

with the submatrices P, Q, R determined by Eq. (5).

We compute mutual information (MI) $I(A:B) = S_A + S_B - S_{AB}$ and logarithmic negativity (LN) $\mathcal{E}_N(\rho_{AB})$, both of which are shown in Fig. 2. MI is a measure of total correlation satisfying $I(A:B)/2 \le E_P(\rho_{AB})$ [10]. LN is a useful probe of quantum entanglement between A and B [38,39], defined as $\mathcal{E}_N(\rho_{AB}) = \log \mathrm{Tr}|\rho_{AB}^{\Gamma_B}|$ [40,41], where $\rho_{AB}^{\Gamma_B}$ is the partial transposition with respect to B. We observe that $\mathcal{E}_N(\rho_{AB})$ takes the largest value at $d = 0$ and for $d \ge 1$ shows exponential decay. On the other hand, MI slowly decreases as function of d (refer to the Supplemental Material [42] for the scaling law of MI and EOP in the conformal limit).

To calculate the EOP, we purify the system by adding auxiliary subsystems $\tilde{A}$ and $\tilde{B}$. Assuming the purified wave functional is Gaussian, we obtain

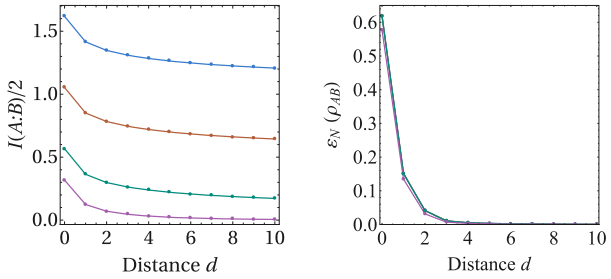

FIG. 2. Half of MI (left) and LN (right) for $|A| = |B| = 4$ and $N = 60$ as a function of d, shown for mass $m = 10^{-1}, 10^{-2}, 10^{-3}, 10^{-4}$ (bottom to top).

$$\Psi_{A\tilde{A}B\tilde{B}}[\phi] = \mathcal{N}_{A\tilde{A}B\tilde{B}}\exp\left(-\frac{1}{2}\phi^{\mathrm{T}}V\phi\right) = \mathcal{N}_{A\tilde{A}B\tilde{B}}\exp\left[-\frac{1}{2}\begin{pmatrix}\phi_{AB}\\ \phi_{\tilde{A}\tilde{B}}\end{pmatrix}^{\mathrm{T}}\begin{pmatrix}J & K\\ K^{\mathrm{T}} & L\end{pmatrix}\begin{pmatrix}\phi_{AB}\\ \phi_{\tilde{A}\tilde{B}}\end{pmatrix}\right], \quad (7)$$

where we have decomposed the matrix V into three submatrices J, K, L. The condition (1) requires $J = P$. Furthermore, assuming subsystems of equal width $w = |A| = |B|$, and setting $|\tilde{A}| = |\tilde{B}| = w$, L becomes a $2w \times 2w$ square matrix and is related to K by the equation

$$L^{-1} = (K^{-1}Q)R^{-1}(K^{-1}Q)^T. \quad (8)$$

Use of a symmetry transformation [36] allows the simplification of the K to the form

$$K = \begin{pmatrix}1_w & K_{A,\tilde{B}}\\ K_{B,\tilde{A}} & 1_w\end{pmatrix}. \quad (9)$$

Thus, all parameters of the purification are contained in the $w \times w$ matrices $K_{A,\tilde{B}}$ and $K_{B,\tilde{A}}$. If one assumes a Z_2 symmetry which reflects $A\tilde{A}$ and $B\tilde{B}$, we will have $K_{A,\tilde{B}} = K^{\mathrm{R}}_{B,\tilde{A}}$, where we define M^R of a matrix M as the inverse ordering of all rows and columns, i.e.,

$$(K^R_{B,\tilde{A}})_{j,k} = (K_{B,\tilde{A}})_{w+1-j,w+1-k}. \quad (10)$$

The Z_2 *asymmetry* $\mathcal{A}$ is defined to quantify the Z_2 symmetry breaking as

$$\mathcal{A} = \|K_{A,\tilde{B}} - K^R_{B,\tilde{A}}\|_2, \quad (11)$$

where $\|M\|_2$ is the two-norm over all entries of M. The actual value of E_P is Z_2 invariant due to $S_{A\tilde{A}} = S_{B\tilde{B}}$.

Then $S_{A\tilde{A}}$ can be computed from the eigenvalue spectrum $\{\lambda_k\}$ of the matrix $\Lambda \equiv -V^{-1}_{A\tilde{A},B\tilde{B}}V_{B\tilde{B},A\tilde{A}}$ [2] as follows:

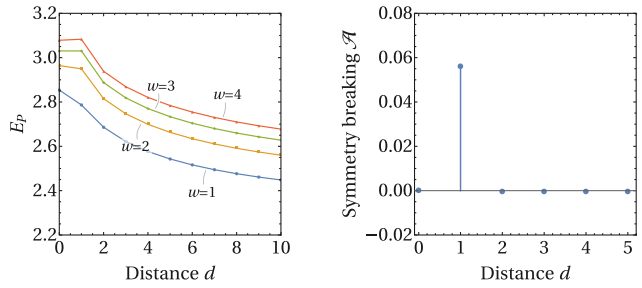

FIG. 3. E_P for $m = 10^{-4}$ and $N = 60$ for various $w = |A| = |B|$ (left) and $\mathcal{A}$ for the data set at $w = 4$ (right).

$$S_{A\tilde{A}} = \sum_k \left(\log \frac{\sqrt{\lambda_k}}{2} + \sqrt{1+\lambda_k} \log \frac{1+\sqrt{1+\lambda_k}}{\lambda_k} \right). \quad (12)$$

The EOP is the minimum of $S_{A\tilde{A}}$ over all purifications $\Psi_{A\tilde{A}B\tilde{B}}[\phi]$, achieved by varying $K_{A,\tilde{B}}$ and $K_{B,\tilde{A}}$. We computed the EOP for subsystem sizes $w = 1$, 2, 3, 4 and studied its dependence on the distance d, using a numerical limited-memory Broyden-Fletcher-Goldfarb-Shanno (L-BFGS) optimization implemented with the C++ package DLIB [43]. Here we made the assumption that an optimal purification is contained in the Gaussian purification above. We also assumed that the auxiliary subsystems have the same sizes as the original ones, and larger numerical setups did not appear to reduce the optimal EOP further. If either assumption were inaccurate, our results for free scalar field theory would only provide an upper bound on the EOP.

As the Z_2 reflection symmetry is a property of the original system ρ_{AB} and leaves the EOP invariant, it might be natural to assume, as in Ref. [36], that the optimal purification is Z_2 symmetric. However, we observe that to find the true minimum of $S_{A\tilde{A}}$, one needs to enlarge the parameter space by breaking the Z_2 exchange symmetry between $A\tilde{A}$ and $B\tilde{B}$. The results for $N = 60$ are shown in Fig. 3 (left). From $d = 0$ to $d = 1$, we observe a plateaulike behavior of E_P at large w whose width appears independent of w, suggesting a finite-size effect. The Z_2 symmetry breaking clearly appears at $d = 1$ (Fig. 3, right). Within numerical accuracy, $\mathcal{A} = 0$ for any $d \neq 1$. This symmetry breaking becomes more pronounced with increasing w. At $w = 1$, it is not observed within our numerical accuracy, while it is clearly visible for $w = 4$.

For small N, the EOP does not monotonically decrease as a function of d (Fig. 4, left). As we increase N, this nonmonotonicity gradually disappears and we get a plateau at large w (Fig. 4, right). It is a surprise that the EOP, being a correlation measure, does not decrease monotonically with distance d, unlike the other correlation measures shown in Fig. 2.

Next, we compute the EOP for spin systems. Let us denote Hilbert space dimension by D such that $D_A = \dim \mathcal{H}_A$ etc. In general, the dimension of auxiliary Hilbert space $D_{\tilde{A}} D_{\tilde{B}}$ should be at least as large as $\mathrm{rank}\rho_{AB}$ to

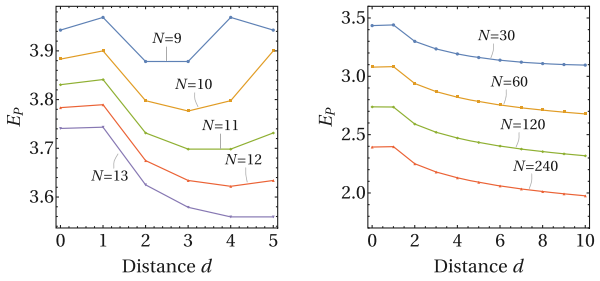

FIG. 4. EOP for small N with block width $w = 2$ and mass $m = 10^{-4}$ (left). EOP for large N with $w = 4$ and $m = 10^{-4}$ (right).

purify a mixed state ρ_{AB}, with no general upper bound. Fortunately, the true minimum of $S_{A\tilde{A}}$ can be found for $D_{\tilde{A}}, D_{\tilde{B}} \leq \mathrm{rank}\rho_{AB}$ in a system with finite-dimensional Hilbert space [44], enabling us to compute EOP in practice. For convenience, we call the purification *minimal* when $D_{\tilde{A}} D_{\tilde{B}} = \mathrm{rank}\rho_{AB}$ and *maximal* when $D_{\tilde{A}} D_{\tilde{B}} = (\mathrm{rank}\rho_{AB})^2$. One example of purification is the thermofield double purification (TFD)

$$|\psi_{\mathrm{TFD}}\rangle_{AB\tilde{A}\tilde{B}} = \sum_i \sqrt{p_i}\, |i\rangle_{AB} |i\rangle_{\tilde{A}\tilde{B}}, \quad (13)$$

where $\rho_{AB} = \sum_i p_i |i\rangle\langle i|_{AB}$ with $\sum_i p_i = 1$, $p_i \geq 0$. All possible purifications of a fixed dimension can be obtained by acting with unitary operators on the auxiliary systems, yielding $|\psi(U)\rangle_{AB\tilde{A}\tilde{B}} = I_{AB} \otimes U_{\tilde{A}\tilde{B}} |\psi_0\rangle_{AB\tilde{A}\tilde{B}}$, where $|\psi_0\rangle_{AB\tilde{A}\tilde{B}}$ is an initial state. We also vary the dimensions $D_{\tilde{A}}, D_{\tilde{B}}$ to achieve both minimal and maximal purification.

We have used a variation of the steepest descent method. To obtain the global minimum, we start from several random initial purifications and ensure that the same point of convergence is reached. Nevertheless, the existence of additional local minima cannot be excluded, in which case the numerical results only provide an upper bound. The same is true for the scalar field case.

We deal with a one-dimensional (1D) transverse-field Ising model

$$H_{\mathrm{Ising}} = -\sum_{\langle i,j \rangle} \sigma_i^z \otimes \sigma_j^z - h \sum_{i=1}^{N} \sigma_i^x, \quad (14)$$

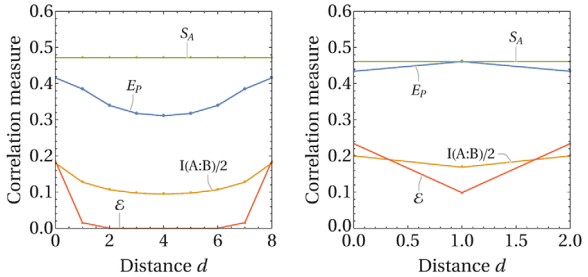

FIG. 5. EOP for $w = 1$, $N = 10$ for the critical Ising model (left). The same for $N = 4$ (right).

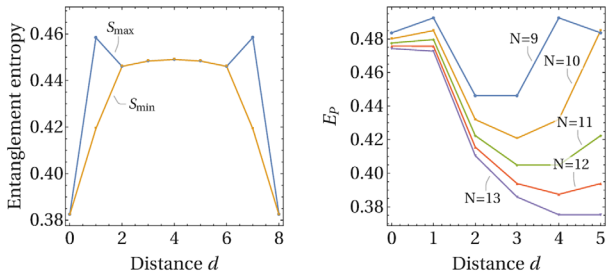

FIG. 6. $S_{\max} = \max\{S_{\tilde{A}}, S_{\tilde{B}}\}$ and $S_{\min} = \min\{S_{\tilde{A}}, S_{\tilde{B}}\}$ of the optimal purifications for $w = 1$ and $N = 10$ (left). The nonmonotonic behavior of EOP for $w = 2$ (right).

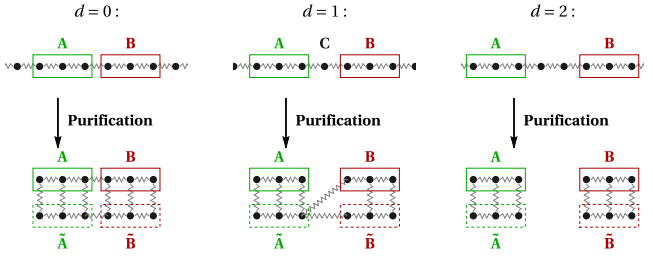

FIG. 7. A toy model for EOP for 1D many body systems, assuming only short-range quantum entanglement (zigzag lines) for $w = |\tilde{A}| = |\tilde{B}| = 3$. At $d = 1$, we only show one of the two optimal Z_2 symmetry-broken purifications.

where $\langle i, j \rangle$ denotes the summation over nearest neighbors with periodic boundary condition. We focus on its ground state at the critical point ($h = 1$) (see the Supplemental Material [42] for noncritical points of the thermal ground state [45,46]). While the optimization is performed using maximal purifications, the optimal purification always corresponds to the minimal purification for this case. The EOP for the corresponding subsystems with $w = |A| = |B| = 1$ as a function of d is depicted in Fig. 5 along with MI and LN. For smaller N ($N = 4$), one can see that the EOP does not decrease with d. This can be explained as follows: E_P must coincide with S_A (Prop. 7 in [47]) at $d = 1$ since ρ_{AB} has support only on a symmetric subspace, while $E_P < S_A$ at $d = 0$ follows from the numerical computation. This provides us with a clear example of EOP increasing with distance. Moreover, the Z_2 symmetry is clearly broken at $d = 1$ as $S_{\tilde{A}} \neq S_{\tilde{B}}$ (Fig. 6, left). For $w = 1$, the Z_2 symmetry is gradually recovered as N gets larger ($N \gtrsim 12$).

We also consider the larger subsystem size $w = 2$. In this case, the EOP is computed using minimal purifications to expedite the computation. We again observe a nonmonotonic behavior of EOP that weakens as N increases (Fig. 6, right) similar to the free scalar case. The Z_2 symmetry breaking is also found at $d = 1$, which remains even at large N.

Finally, we seek to provide an interpretation of our results. For both free scalar theory and the critical Ising model, we observed a nonmonotonic or plateaulike behavior of the EOP at small d. These behaviors are very special to EOP and do not appear in MI. This is in contrast to the fact that they possess similar information-theoretic properties as total correlation measures (refer to, e.g., Ref. [10]). This mirrors the observation in Refs. [11,12] that the value of holographic EOP behaves differently than that of holographic MI, with the former developing a plateaulike behavior.

Suppose total correlations (measured by half of MI) are a combination of quantum entanglement and classical correlations. As $E_P \geq 2(I(A:B)/2)$ for separable states [9] while $E_P = I/2$ for pure states, we assert that EOP enhances the classical correlations compared to $I(A:B)/2$ at least twofold, while treating quantum entanglement equivalently. This explains the nonmonotonicity of EOP as well: quantum entanglement can be estimated by the LN, which falls of quickly with d. Thus, classical contributions at $d \geq 1$ are enhanced compared to short-range quantum entanglement at $d = 0$. Possible connections to analogous quantities such as quantum discord [48,49] will be an interesting future work.

We also propose a mechanism of Z_2 symmetry breaking at $d = 1$ by a toy model with dominant nearest-neighbor quantum entanglement (Fig. 7). The distinction between quantum entanglement and classical correlation is crucial here, as well. At $d = 1$, an intermediate site C is strongly entangled with both A and B, and tracing it out turns ρ_{AB} into a highly mixed state. This leads to strong classical correlations between A and B. As a result, the purification requires strong entanglement for $A \leftrightarrow \tilde{A}$, $B \leftrightarrow \tilde{B}$, $\tilde{A} \leftrightarrow \tilde{B}$, $\tilde{A} \leftrightarrow B$ and $A \leftrightarrow \tilde{B}$ in order to convert the large amount of classical correlations into quantum entanglement. This complicated competition, under the constraint of monogamy, results in a Z_2 reflection symmetry breaking, where only either $\tilde{A} \leftrightarrow B$ or $A \leftrightarrow \tilde{B}$ exhibits strong entanglement (Fig. 7, center). This picture is indeed confirmed both for the free scalar and the Ising model. In contrast, correlations are either weak at $d \geq 2$ or are strong but mainly consist of entanglement at $d = 0$. Both cases require little purification, allowing a simple symmetric purification to be optimal. This suggests that the Z_2 symmetry breaking occurs when ρ_{AB} possesses strong classical correlations.

Notice that the Z_2 symmetry breaking does not occur for CFT vacua in holographic setups. However, such a symmetry breaking can be possible in holography for excited states or nonconformal setups. Searching for Z_2 symmetry breaking in holographic EOP will thus serve as an interesting future endeavor.

We thank Pawel Caputa, Horacio Casini, Jens Eisert, Masamichi Miyaji, Masahiro Nozaki, Kazuma Shimizu, and Brian Swingle for useful conversations. We are very grateful to Yoshifumi Nakata for valuable comments on the draft. A. B. and K. U. are supported by JSPS Fellowships.

A. J. is supported by a *Studienstiftung* Fellowship. T. T. is supported by the Simons Foundation through the "It from Qubit" collaboration. T. T. is supported by JSPS Grant-in-Aid for Scientific Research (A) Grant No. 16H02182 and by JSPS Grant-in-Aid for Challenging Research (Exploratory) Grant No. 18K18766. A. B. and T. T. are supported by JSPS Grant-in-Aid for JSPS Fellows Grant No. 17F17023. K. U. is supported by Grant-in-Aid for JSPS Fellows Grant No. 18J22888. T. T. is also supported by World Premier International Research Center Initiative from the Japan Ministry of Education, Culture, Sports, Science and Technology.

[1] M. J. Donald, M. Horodecki, and O. Rudolph, The uniqueness theorem for entanglement measures, J. Math. Phys. (N.Y.) **43**, 4252 (2002).
[2] L. Bombelli, R. K. Koul, J. Lee, and R. D. Sorkin, A quantum source of entropy for black holes, Phys. Rev. D **34**, 373 (1986).
[3] M. Srednicki, Entropy and Area, Phys. Rev. Lett. **71**, 666 (1993).
[4] C. Holzhey, F. Larsen, and F. Wilczek, Geometric and renormalized entropy in conformal field theory, Nucl. Phys. **B424**, 443 (1994).
[5] J. M. Maldacena, The large N limit of superconformal field theories and supergravity, Int. J. Theor. Phys. **38**, 1113 (1999); Adv. Theor. Math. Phys. **2**, 231 (1998).
[6] S. Ryu and T. Takayanagi, Holographic Derivation of Entanglement Entropy from AdS/CFT, Phys. Rev. Lett. **96**, 181602 (2006); Aspects of holographic entanglement entropy, J. High Energy Phys. 08 (2006) 045.
[7] V. E. Hubeny, M. Rangamani, and T. Takayanagi, A covariant holographic entanglement entropy proposal, J. High Energy Phys. 07 (**2007**) 062.
[8] R. Horodecki, P. Horodecki, M. Horodecki, and K. Horodecki, Quantum entanglement, Rev. Mod. Phys. **81**, 865 (2009).
[9] B. M. Terhal, M. Horodecki, D. W. Leung, and D. P. DiVincenzo, The entanglement of purification, J. Math. Phys. (N.Y.) **43**, 4286 (2002).
[10] S. Bagchi and A. K. Pati, Monogamy, polygamy, and other properties of entanglement of purification, Phys. Rev. A **91**, 042323 (2015).
[11] K. Umemoto and T. Takayanagi, Entanglement of purification through holographic duality, Nat. Phys. **14**, 573 (2018).
[12] P. Nguyen, T. Devakul, M. G. Halbasch, M. P. Zaletel, and B. Swingle, Entanglement of purification: From spin chains to holography, J. High Energy Phys. 01 (2018) 098.
[13] P. Caputa, M. Miyaji, T. Takayanagi, and K. Umemoto, Holographic Entanglement of Purification from Conformal Field Theories, Phys. Rev. Lett. **122**, 111601 (2019).
[14] N. Bao and I. F. Halpern, Holographic inequalities and entanglement of purification, J. High Energy Phys. 03 (2018) 006.
[15] D. Blanco, M. Leston, and G. Perez-Nadal, Gravity from entanglement for boundary subregions, J. High Energy Phys. 06 (2018) 130.
[16] H. Hirai, K. Tamaoka, and T. Yokoya, Towards entanglement of purification for conformal field theories, Prog. Theor. Exp. Phys. (**2018**), 063B03.
[17] R. Espindola, A. Guijosa, and J. F. Pedraza, Entanglement wedge reconstruction and entanglement of purification, Eur. Phys. J. C **78**, 646 (2018).
[18] N. Bao and I. F. Halpern, Conditional and multipartite entanglements of purification and holography, Phys. Rev. D **99**, 046010 (2019).
[19] Y. Nomura, P. Rath, and N. Salzetta, Pulling the boundary into the bulk, Phys. Rev. D **98**, 026010 (2018).
[20] K. Umemoto and Y. Zhou, Entanglement of purification for multipartite states and its holographic dual, J. High Energy Phys. 10 (2018) 152.
[21] R. Abt, J. Erdmenger, M. Gerbershagen, C. M. Melby-Thompson, and C. Northe, Holographic subregion complexity from kinematic space, J. High Energy Phys. 01 (2019) 012.
[22] A. May and E. Hijano, The holographic entropy zoo, J. High Energy Phys. 10 (2018) 036.
[23] Y. Chen, X. Dong, A. Lewkowycz, and X. L. Qi, Modular flow as a disentangler, J. High Energy Phys. 12 (2018) 083.
[24] J. Kudler-Flam and S. Ryu, Entanglement negativity and minimal entanglement wedge cross sections in holographic theories, arXiv:1808.00446.
[25] S. X. Cui, P. Hayden, T. He, M. Headrick, B. Stoica, and M. Walter, Bit threads and holographic monogamy, arXiv:1808.05234.
[26] V. E. Hubeny, Bulk locality and cooperative flows, J. High Energy Phys. 12 (2018) 068.
[27] K. Tamaoka, Entanglement Wedge Cross Section from the Dual Density Matrix, Phys. Rev. Lett. **122**, 141601 (2019).
[28] J. C. Cresswell, I. T. Jardine, and A. W. Peet, Holographic relations for OPE blocks in excited states, J. High Energy Phys. 03 (2019) 058.
[29] E. Caceres and M. L. Xiao, Complexity-action of singular subregions, J. High Energy Phys. 03 (2019) 062.
[30] R. Q. Yang, C. Y. Zhang, and W. M. Li, Holographic entanglement of purification for thermofield double states and thermal quench, J. High Energy Phys. 01 (2019) 114.
[31] N. Bao, A. Chatwin-Davies, and G. N. Remmen, Entanglement of purification and multiboundary wormhole geometries, J. High Energy Phys. 02 (2019) 110.
[32] N. Bao, Minimal purifications, wormhole geometries, and the complexity = action proposal, arXiv:1811.03113.
[33] C. A. Agon, J. de Boer, and J. F. Pedraza, Geometric aspects of holographic bit threads, arXiv:1811.08879.
[34] N. Bao, G. Penington, J. Sorce, and A. Wall, Beyond toy models: Distilling tensor networks in full AdS/CFT, arXiv:1812.01171.
[35] Wu-zhong Guo, Entanglement of purification and projective measurement in CFT, arXiv:1901.00330.
[36] A. Bhattacharyya, T. Takayanagi, and K. Umemoto, Entanglement of purification in free scalar field theories, J. High Energy Phys. 04 (2018) 132.
[37] N. Shiba, Entanglement entropy of two black holes and entanglement entropic force, Phys. Rev. D **83**, 065002 (2011); N. Shiba, Entanglement entropy of two spheres, J. High Energy Phys. 07 (2012) 100; N. Shiba and

T. Takayanagi, Volume law for the entanglement entropy in non-local QFTs, J. High Energy Phys. 02 (2014) 033.
[38] J. Eisert, Entanglement in quantum information theory, Ph.D. thesis, University of Potsdam, 2001.
[39] K. Audenaert, J. Eisert, M. B. Plenio, and R. F. Werner, Entanglement properties of the harmonic chain, Phys. Rev. A **66**, 042327 (2002).
[40] G. Vidal and R. F. Werner, A computable measure of entanglement, Phys. Rev. A **65**, 032314 (2002).
[41] M. B. Plenio, Logarithmic Negativity: A Full Entanglement Monotone that is not Convex, Phys. Rev. Lett. **95**, 090503 (2005).
[42] See Supplemental Material at http://link.aps.org/supplemental/10.1103/PhysRevLett.122.201601 for the scaling law of MI and EOP in the conformal limit or for the EOP in the noncritical Ising model.
[43] D. King, DLIB C++ Library, http://dlib.net.
[44] B. Ibinson, N. Linden, and A. Winter, Robustness of quantum Markov chains, Commun. Math. Phys. **277**, 289 (2007).
[45] P. Pfeuty, The one-dimensional Ising model with a transverse field, Ann. Phys. **57**, 79 (1970).
[46] T. J. Osborne and M. A. Nielsen, Entanglement in a simple quantum phase transition, Phys. Rev. A **66**, 032110 (2002).
[47] M. Christandl and A. Winter, Uncertainty, monogamy, and locking of quantum correlations, IEEE Trans. Inf. Theory **51**, 3159 (2005).
[48] L. Henderson and V. Vedral, Classical, quantum and total correlations, J. Phys. A **34**, 6899 (2001).
[49] H. Ollivier and W. H. Zurek, Quantum Discord: A Measure of the Quantumness of Correlations, Phys. Rev. Lett. **88**, 017901 (2001).